

## Effect of toroidal flow and flow shear on the quasi-interchange instability in tokamaks with weak magnetic shear

C. Wahlberg

*Department of Astronomy and Space Physics, EURATOM/VR Fusion Association,  
P.O. Box 515, Uppsala University, SE-751 20 Uppsala, Sweden*

Introduction Tokamak experiments in the “hybrid” scenario [1], as well as some experiments in spherical tokamaks [2], have  $q$ -values very close to unity in a wide area in the plasma core. Static, toroidal equilibria of this kind are susceptible to a pressure-driven, internal kink instability with an eigenfunction of “quasi-interchange” character [3]. In many experiments (especially in spherical tokamaks) the toroidal plasma rotation driven by the neutral beams is, however, quite substantial [1-2]. It is therefore of interest to examine the consequences of such plasma flows for the quasi-interchange (QI) instability. The present work investigates the effect of toroidal flow and, especially, toroidal flow shear on the QI mode using a compressible, ideal MHD description of the plasma. The work extends the analysis in Ref. [4], where weakly subsonic, rigid rotation was found to be strongly stabilizing.

Equilibrium We consider a toroidal plasma with circular cross section and large aspect ratio,  $\varepsilon = r/R_0 \ll 1$ , where  $r$  is the minor radius in the plasma and  $R_0$  the major radius of the plasma center. Furthermore, we assume that the plasma rotates toroidally with a frequency of order  $\Omega \sim \omega_s \sim \varepsilon\omega_A$ , where  $\omega_s = (\Gamma p_0 / \rho_0)^{1/2} / R_0$  is the sound frequency and  $\omega_A = B_0 / R_0 (\mu_0 \rho_0)^{1/2}$  the Alfvén frequency ( $p_0$  and  $\rho_0$  denote the plasma pressure and density, respectively,  $B_0$  the toroidal magnetic field and  $\Gamma = 5/3$  the adiabatic index). Assuming that the equilibrium magnetic surfaces are isothermal, the Shafranov shift  $\Delta$  is described by the equation [4]  $d\Delta/dr = -r(\beta_p + l_i/2)/R_0$ , with the plasma inductance  $l_i$  and the poloidal beta value  $\beta_p$  given by

$$l_i(r) = \frac{2q^2}{r^4} \int_0^r \frac{r'^3}{q^2} dr', \quad \beta_p(r) = -\frac{2\mu_0 q^2 R_0^2}{r^4 B_0^2} \int_0^r r'^2 \frac{d}{dr'} (p_0 + M_s^2 p_0) dr', \quad (1a, b)$$

respectively.  $M_s = (\rho_0 \Omega^2 R_0^2 / 2p_0)^{1/2}$  in Eq. (1b) is the sonic Mach number. Thus, the rotation contributes to the Shafranov shift by increasing the “effective” poloidal beta value. When  $M_s \sim 1$ , the effect of the dynamical pressure  $M_s^2 p_0 = \rho_0 \Omega^2 R_0^2 / 2$  is of the same order of magnitude as the effect of the static pressure. Here we specify the equilibrium profiles as follows: We let  $q = 1$  in the region  $0 \leq r \leq r_1$  of weak magnetic shear, whereas in the edge region  $r_1 \leq r \leq a$  we assume that  $q(r)$  increases quadratically

with  $r$  from unity at  $r = r_1$  up to  $q_a = 4$  at the plasma edge  $r = a$  [4]. Furthermore,  $\rho_0(r)$  is assumed constant, and  $p_0(r)$  and  $\Omega(r)$  are chosen as

$$p_0(r) = p_0(0)(1 - r^2/a^2), \quad \Omega(r) = \Omega_0(1 - r^2/r_\Omega^2)^{1/2}. \quad (2a, b)$$

This leads to a constant value of  $\beta_p$  in the region  $0 \leq r \leq r_1$ . More specifically, we obtain the effective (total) beta value as  $\beta_p = \beta_{p0} + \beta_{p\Omega}$ , where the static and dynamical parts of  $\beta_p$  are given by  $\beta_{p0} = \mu_0 p_0(0) R_0^2 / a^2 B_0^2$  and  $\beta_{p\Omega} = \Omega_0^2 R_0^2 / 2\omega_A^2 r_\Omega^2$ , respectively. Examples of the  $q$ - and  $\Omega$ -profiles used here are shown in Fig. 1. The rotation shear is described by the parameter  $r_\Omega$ , which is allowed to vary in the range  $r_1 \leq r_\Omega \leq \infty$ . We point out that the rotation profile is of importance only in the region of weak magnetic shear, so the dashed parts of the  $\Omega$ -curves in Fig. 1 are redundant for the QI stability problem looked at here. With other forms of the profiles of  $\rho_0(r)$ ,  $p_0(r)$  and  $\Omega(r)$  we expect quantitative, but not qualitative, differences from the results of the stability analysis below.

**Stability analysis** Since the pressure- and rotation-profiles in Eqs. (2a, b) lead to a constant  $\beta_p = \beta_{p0} + \beta_{p\Omega}$  in the region of weak magnetic shear, the stability equation for the QI mode derived for a rigidly rotating plasma in Ref. [4] is valid also here. Thus, neglecting the second term in the inertia operator in Eq. (9b) in Ref. [4], the stability problem of the QI mode for the profiles in Eqs. (2a, b) can be formulated as [4]

$$\int_0^{\hat{r}_1} \frac{\hat{r}^5 d\hat{r}}{Q(\hat{r}, \omega)} = \frac{\hat{r}_1^4}{\beta_p^2} \frac{1-C}{3+C}, \quad \text{where } Q = -\hat{\omega}_D^2 + \hat{\Omega}^2 M_s^2 - \frac{(4\hat{\omega}_D^2 + \hat{\Omega}^2/2)\hat{\Omega}^2 + 2\hat{\omega}_D^2\hat{\omega}_s^2}{\hat{\omega}_s^2 - \hat{\omega}_D^2}. \quad (3a, b)$$

Here,  $C$  is a numerical constant related to the solution of the  $m = 2$  side-band equation in the edge region [4],  $\omega_D(r) \equiv \omega + \Omega(r)$  is the Doppler-shifted mode frequency, and the normalized quantities in (3) are defined as  $\hat{r} = r/a$ ,  $\hat{\omega}_D = \omega_D / \varepsilon_a \omega_A$ ,  $\hat{\omega}_s = \omega_s / \varepsilon_a \omega_A$ ,  $\hat{\Omega} = \Omega / \varepsilon_a \omega_A$ , where  $\varepsilon_a = a/R_0$ . In addition to  $\omega_D(r)$  and  $\Omega(r)$ ,  $r$ -dependence of  $Q(\hat{r}, \omega)$  comes from  $\hat{\omega}_s^2 = \Gamma \beta_{p0} (1 - \hat{r}^2)$  and  $M_s^2 = \hat{\Omega}_0^2 (1 - \hat{r}^2 / \hat{r}_\Omega^2) / 2\beta_{p0} (1 - \hat{r}^2)$ .

In the present work, the eigenvalue equation (3) has been solved numerically, and the main features of the eigenfrequency  $\omega$  are illustrated in Figs. 2-6. Two main regimes (and mechanisms) of rotational stabilization of the QI instability can be identified. Firstly, if the rotation is rigid or weakly sheared ( $r_1/r_\Omega \sim 2/3$  or smaller, see Fig. 1), the QI mode is stabilized by the Brunt-Väisälä (BV) mechanism explained in Ref. [4]. This is shown in Fig. 2 which illustrates the complex eigenvalue  $\omega = \omega_r + i\omega_i$  (in normalized form) as a function of the (normalized) rotation frequency at the axis for the plasma parameters  $r_1 = 0.5a$ ,  $\beta_{p0} = 0.3$  and  $r_\Omega = a$ . Notice the splitting of  $\omega_r$  (represented by the Doppler-shifted mode frequency at the magnetic axis) at the point of BV-stabilization. Secondly, if the rotation is strongly sheared ( $r_1/r_\Omega \sim 1$ ), a substantial reduction of the

growth rate takes place already for central rotation frequencies smaller than the rigid rotation frequency required for BV-stabilization. The dependence of  $\omega_r$  and  $\omega_i$  on the central rotation frequency in such a case is illustrated in Fig. 3 for a plasma with  $r_1 = 0.2a$ ,  $\beta_{p0} = 0.3$  and  $r_\Omega = 0.225a$ . Notice that there is no splitting of  $\omega_r$  (dashed, blue curve) in this case (no BV effect) and that there is a limited range of  $\Omega_0$  that gives a reduced growth rate  $\omega_i$  (solid, red curve). Fig. 4 illustrates the growth rate and the loss of BV-stabilization (solid, red curves) in a plasma with the same parameters as in Fig. 2 as the shear increases from  $r_\Omega/a = 1000$  ( $\approx$  rigid rotation) up to  $r_\Omega/a = 0.6$ . As the flow shear becomes of order  $r_1/r_\Omega \sim 1$ , however, the growth rate is very strongly reduced, as shown by the dotted, green curve in the figure, calculated for  $r_\Omega/a = 0.51$ . This shear stabilization is, however, lost already for  $r_\Omega/a > 0.52$ - $0.53$ . Fig. 5 illustrates the same effect in the case  $r_1 = 0.2a$ . Finally, the  $\beta_{p0}$ -dependence of the critical rotation frequency for BV-stabilization of the QI mode in the case of weak, or moderate, flow shear for both  $r_1/a = 0.2$  and  $r_1/a = 0.5$  is shown in Fig. 6. Notice that  $\Omega_{0,crit}$  is normalized with the width  $r_1$  of the region of low magnetic shear, leading to approximately similar stability boundaries for the two cases  $r_1/a = 0.2$  (red) and  $r_1/a = 0.5$  (blue). This is due to the scaling  $\Omega_{0,crit} \sim r_1$  found in the case of rigid rotation in Ref. [4], which is seen to be (approximately) valid also if the rotation is weakly sheared. Furthermore, the  $\beta_{p0}$ -scaling  $\Omega_{0,crit} \sim \beta_{p0}^{3/4}$  of the critical rotation frequency, strictly valid in the case of rigid rotation [4], is fairly accurate also for weakly sheared rotation.

Conclusions It has been shown that the Brunt-Väisälä mechanism, discussed in detail in Ref. [4], is capable of stabilizing the quasi-interchange instability in tokamaks with  $q \approx 1$  in the plasma core also if the toroidal rotation is weakly sheared. Since the flow shear leads to an enhanced “effective” poloidal beta value  $\beta_p$  (static plus dynamic), however, weakly sheared rotation requires somewhat higher central rotation frequencies for stabilization as compared with rigid rotation. At sufficiently strong flow shear, Brunt-Väisälä stabilization is in general not possible for reasonable central rotation frequencies. On the other hand, if the rotation is very strongly sheared ( $r_1/r_\Omega \sim 1$ ), the shear itself is capable of reducing the growth rate of the instability to very small values.

- [1] Litaudon X *et al* 2004 *Plasma Phys. Control. Fusion* **46** A19
- [2] Menard J E *et al* 2003 *Nucl. Fusion* **43** 330, and *Proc. 30th EPS Conf. on Contr. Fusion and Plasma Phys. (St Petersburg, 2003)* vol 27A, P-3.101
- [3] Wesson J A 1986 *Plasma Phys. Control. Fusion* **28** 243; Hastie R J and Hender T C 1988 *Nucl. Fusion* **28** 585; Waelbroeck F L and Hazeltine R D 1988 *Phys. Fluids* **31** 1217
- [4] Wahlberg C 2005 *Plasma Phys. Control. Fusion* **47** 757

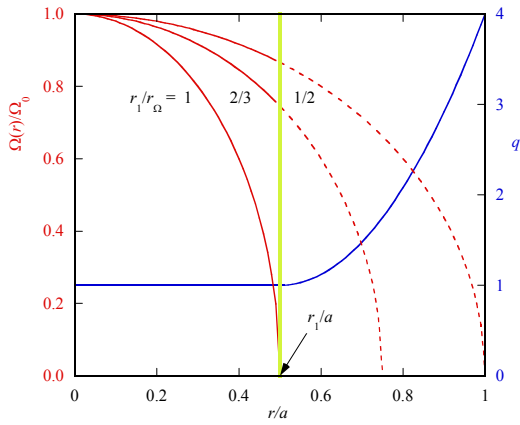


Fig.1 Examples of the rotation ( $\Omega$ ) profile and the  $q$ -profile used in the numerical solution of the eigenvalue equation (3).

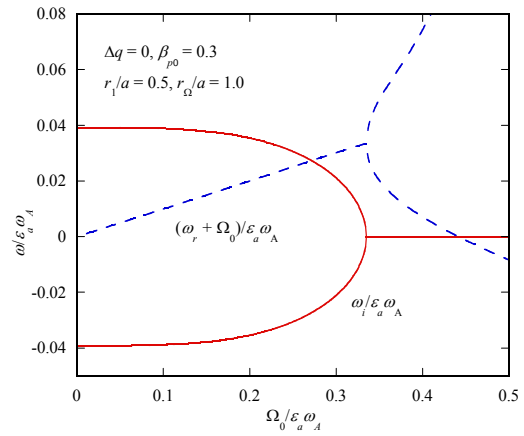


Fig. 2 The real (dashed) and imaginary (solid) parts of the eigenvalue  $\omega$  as functions of  $\Omega_0$ . The figure illustrates the stabilization of the mode by the Brunt-Väisälä mechanism.

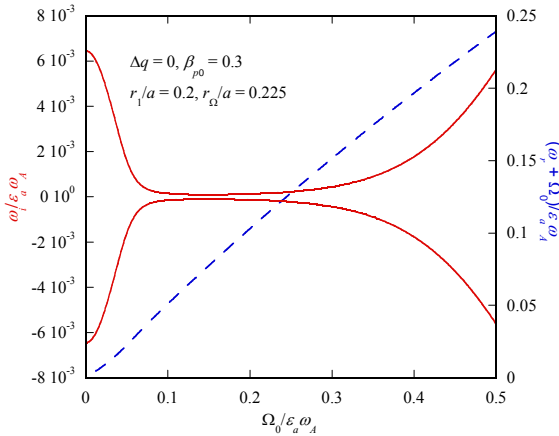


Fig. 3 The real (dashed) and imaginary (solid) parts of the eigenvalue  $\omega$  as functions of  $\Omega_0$ . The figure illustrates the reduction of the growth rate by very strong flow shear.

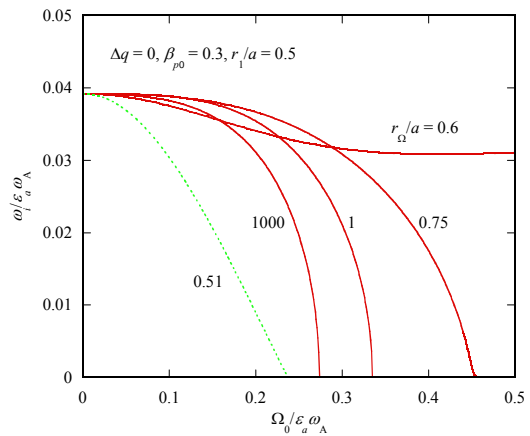


Fig. 4 Growth rate as a function of  $\Omega_0$  for various values of the flow-shear parameter  $r_{\Omega}/a$ . The solid (red) curves with  $r_{\Omega}/a \geq 0.75$  correspond to Brunt-Väisälä stabilization and the dotted (green) curve to shear stabilization

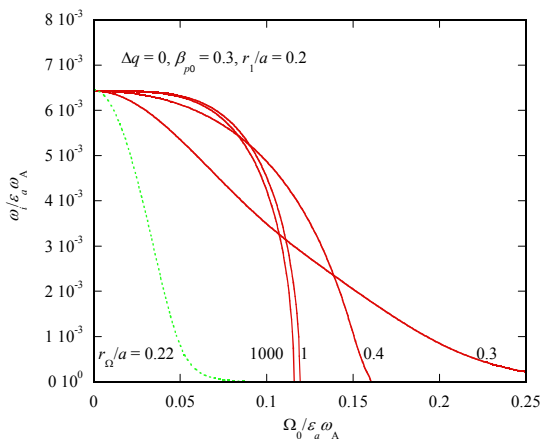


Fig. 5 Growth rate as a function of  $\Omega_0$  for various values of the flow-shear parameter  $r_{\Omega}/a$ . The solid (red) curves with  $r_{\Omega}/a \geq 0.4$  correspond to Brunt-Väisälä stabilization and the dotted (green) curve to shear stabilization

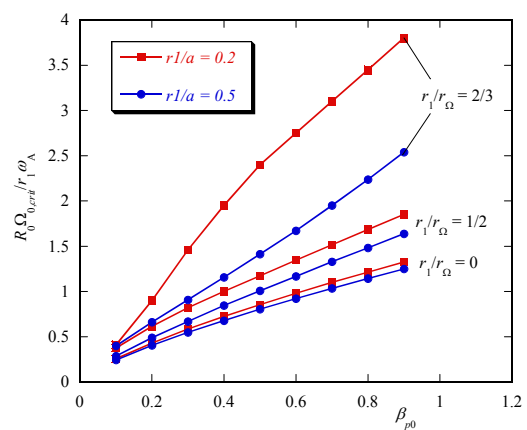


Fig. 6 Critical rotation frequency as a function of  $\beta_{p0}$  for a few values of the flow-shear parameter  $r_{\Omega}/a$  and for  $r_1/a = 0.2$  (red) and  $r_1/a = 0.5$  (blue).